Journal of Materials Chemistry C

PAPER

View Article Online
View Journal | View Issue

Cite this: J. Mater. Chem. C, 2019, 7, 1370

Diazaspirocycles: novel platforms for efficient phosphorescent organic light-emitting diodes†

Xiang-Yang Liu,‡ Yi-Jie Zhang,‡ Xiyu Fei, Quan Ran, Man-Keung Fung * and Jian Fan *

Received 30th October 2018,
Accepted 24th December 2018

DOI: 10.1039/c8tc05462b

rsc.li/materials-c

Azafluorenone was discovered decades ago and its derivatives have received widespread attention in various research fields. However, the application of azafluorenone and its derivatives in organic light-emitting diode (OLED) materials is rarely reported and the related device performance is still not satisfactory. In this work, 1,4-diazafluorenone and its two analogues were prepared as precursors and three novel spiro compounds, **SAIP**, **SAIQ**, and **SABIQ**, were synthesized. The basic physical and chemical properties of **SAIP**, **SAIQ**, and **SABIQ** were studied in detail. From **SAIP** to **SAIQ** and **SABIQ**, the triplet energies (E_Ts) and optical band gaps (E_gs) decrease gradually with the extension of the intramolecular conjugation length. In addition, blue/green/red and green/red phosphorescent OLEDs (PHOLEDs) were fabricated with **SAIP** and **SAIQ** as host materials, respectively. It is worth noting that all green and red devices based on **SAIP** or **SAIQ** showed a relatively high device performance with maximum external quantum efficiencies (EQEs) of 17.8% and 21.4%, respectively. These results further show the high potential of azafluorenone and its analogues in the building of efficient host materials.

Introduction

The chemistry of azafluorenones (Fig. 1) has been well studied in the early literature,[1] and there has been significant development in the synthetic methods for these fused ring systems over the last four decades. A survey of the preparation of azafluorenones shows that there are three typical synthetic routes. The first one is to make use of oxidative ring contractions of nitrogen-containing fused compounds. For example, azafluorenone derivatives can be obtained by oxidation of the corresponding substituted azaphenanthrenes with potassium permanganate ($KMnO_4$).[1b,2] The second method is to increase the number of fused rings by annelation of the heterocycle. For instance, the condensation of the indane–1,3-dione-aminocrotonate–aldehyde three-component system is the most efficient and therefore widely used for the synthesis of 1,4-dihydro-4-azafluorenes,[3] which can be easily aromatized with oxidants or under UV irradiation to obtain the corresponding 4-azafluorenones.[4] The third method is intramolecular cyclocondensation of aryl- or aroyl pyridines. The availability of diverse pyridine derivatives (phenylpyridinecarboxylic acids,[5] and respective acid chlorides,[6] nitriles, esters[5e,f,7] and acid amides[8]) has offered broad possibilities for the synthesis of all isomeric azafluorenones. The corresponding cyclisation often requires sulfuric[9] and polyphosphoric acids (PPAs),[7d,10] aluminum chloride ($AlCl_3$),[11] and some other compounds[5e,f,8,12] as condensing agents. Other specific methods such as the photochemical Pschorr cyclization of 2-diazoniodiaryl ketones,[13] radical Pschorr cyclization of organoboronic acids and trifluoroborates,[14] gas-phase thermolysis of diazo compounds,[1b] intramolecular Heck reactions of 3-aroylpyridines,[15] intramolecular carbonylation *via* oxidative C–H functionalization of the methyl group,[16] and C–H functionalization of the methyl/hydroxymethyl/aldehyde group[17] have also been reported.

Recently, various nitrogenated rigid molecular building blocks[18] such as carbazole,[19] dibenzo[*b*,*d*]furan (DBF),[20] dibenzo[*b*,*d*]thiophene (DBT),[21] and 9,9′-spirobifluorene (SBF)[22] have

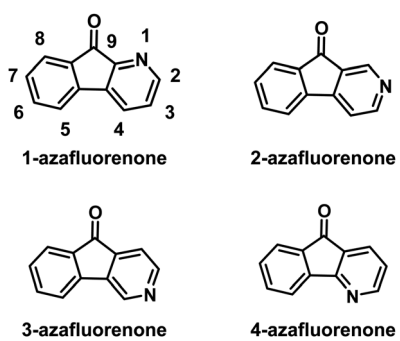

Fig. 1 The structures of isomeric azafluorenones.

Institute of Functional Nano & Soft Materials (FUNSOM), Jiangsu Key Laboratory for Carbon-Based Functional Materials & Devices, Soochow University, Suzhou, Jiangsu 215123, China. E-mail: mkfung@suda.edu.cn, jianfan@suda.edu.cn

† Electronic supplementary information (ESI) available. See DOI: 10.1039/c8tc05462b

‡ These two authors contributed equally to this paper.

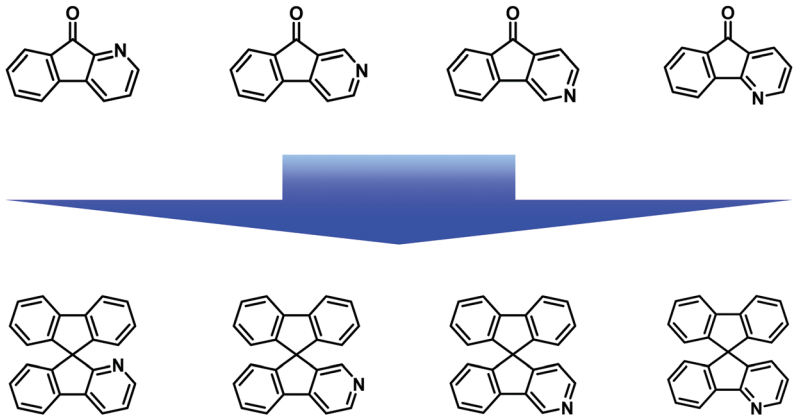

Fig. 2 Reported structures of azafluorenones and the corresponding azaspirobifluorenes.

been extensively used as functional materials in organic light-emitting diodes (OLEDs).[19b–g,20,21,22a–e] Many research studies have illustrated that the introduction of an sp^2 nitrogen atom into the backbone of organic conjugated materials can improve their electron transport ability.[18] For this purpose, azafluorenones (Fig. 2) and diazafluorenones (Fig. 3) are good starting materials to construct the corresponding aza-SBF derivatives.[23–25] It is worth noting that 4,5-diaza-SBF derivatives have been more extensively studied[22c–f,23] relative to other diaza-SBF compounds. There are several reported ways to synthesize diazafluorenones, including the ring contraction reactions of phenanthrolinchinones,[2d,26] the condensation reaction of ninhydrin/aryl methyl ketone and hydrazine hydrate,[23,27] the condensation reaction of 1-(*N*,*N*-dimethylaminomethyliden)indan-2-one and benzamidine hydrochloride hydrate,[28] and the cyclocondensation reaction of ninhydrin and ethylenediamine.[29]

In OLEDs, phosphorescent emitters are normally doped into suitable host materials to suppress the competitive decay process such as triplet–triplet annihilation and triplet–polaron annihilation.[30] Therefore, the chemical and physical properties of the host materials such as good thermal stability, suitable triplet energy, and balance charge transfer properties are important for fabricating efficient phosphorescent OLEDs (PHOLEDs).[31] Very recently, plenty of work has been reported on the development of highly efficient host materials for blue, green, and red PHOLEDs,[32] as well as the optimization of the device structure.[33] For instance, Liao and co-workers reported a novel thermally activated delayed fluorescence (TADF) material as the host material for a red PHOLED with an external quantum efficiency (EQE) over 31%.[32e] So far, many novel molecular platforms such as dispiro,[32a] propellane[32a] and 9-silafluorene[32b] have been used for the construction of highly efficient host materials. On the other hand, high performance PHOLEDs have also been realized *via* device optimization such as applying a co-host,[33a,b] a double emission layer,[33c] and a novel electron-transporting material.[33d,e]

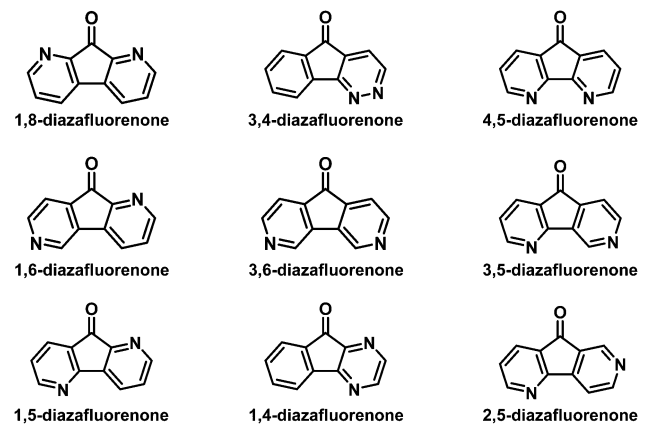

Fig. 3 Reported structures of diazafluorenones.

To develop high performance host materials, several empirical design strategies that would improve the charge transport capability of aza-SBFs have been reported in recent years, such as introduction of aromatic amine substituents (diphenylamine, carbazole, *etc.*) to aza-SBF backbones[34] and the replacement of fluorene with a triphenylamine or diphenylsulfane unit.[35] In this article, three novel spirocycles, 10-phenyl-10*H*-spiro[acridine-9,9′-indeno[1,2-*b*]pyrazine] (**SAIP**), 10-phenyl-10*H*-spiro[acridine-9,11′-indeno[1,2-*b*]quinoxaline] (**SAIQ**) and 10-phenyl-10*H*-spiro[acridine-9,13′-benzo[*g*]indeno[1,2-*b*]-quinoxaline] (**SABIQ**), are constructed. Basic properties such as the thermal and photophysical properties and the electrochemistry behaviors of **SAIP**, **SAIQ**, and **SABIQ** were fully characterized. The introduction of different electron acceptor segments has a great influence on the basic physical and chemistry properties of these spirocycles, but has a minor effect on their electroluminescence performance. Blue, green, and red PHOLEDs were fabricated with bis(4,6-(difluorophenyl)pyridinato-*N*,$C^{2'}$)picolinate iridium(III) (FIrpic), bis(2-phenylpyridine)(acetylacetonate)iridium(III) ($Ir(ppy)_2$(acac)), and bis(2-methyldibenzo-[*f*,*h*]-quinoxaline)iridium(III) (acetylacetonate) ($Ir(MDQ)_2$(acac)) as dopants, respectively. To our great delight, the green and red devices demonstrated moderate device performance with external quantum efficiencies above 17% and 21%, respectively.

Experimental section

Materials synthesis

The precursors 1,4-diazafluorenone (**1**),[29] 11*H*-indeno[1,2-*b*]quinoxalin-11-one (**2**),[36] and 13*H*-benzo[*g*]indeno[1,2-*b*]quinoxalin-13-one (**3**)[37] were prepared in accordance with literature methods.

1,4-Diazafluorenone (1). ^{1}H NMR (400 MHz, chloroform-*d*) δ 8.56–8.52 (m, 1H), 8.50–8.47 (m, 1H), 7.89 (d, J = 7.5 Hz, 1H), 7.82 (d, J = 7.4 Hz, 1H), 7.68 (t, J = 7.6 Hz, 1H), 7.53 (t, J = 7.5 Hz, 1H) ppm.

11*H*-Indeno[1,2-*b*]quinoxalin-11-one (2). ^{1}H NMR (400 MHz, chloroform-*d*) δ 8.24 (d, J = 8.3 Hz, 1H), 8.14–8.08 (m, 2H), 7.93 (d, J = 7.5 Hz, 1H), 7.87–7.71 (m, 3H), 7.61 (t, J = 7.5 Hz, 1H) ppm.

13*H*-Benzo[*g*]indeno[1,2-*b*]quinoxalin-13-one (3). ^{1}H NMR (400 MHz, chloroform-*d*) δ 8.79 (s, 1H), 8.62 (s, 1H), 8.20 (d, J = 7.6 Hz, 1H), 8.09 (t, J = 8.7 Hz, 2H), 7.98 (d, J = 7.6 Hz, 1H), 7.82 (t, J = 7.5 Hz, 1H), 7.69–7.55 (m, 3H) ppm.

10-Phenyl-10*H*-spiro[acridine-9,9′-indeno[1,2-*b*]pyrazine] (SAIP). 2-Bromo-*N*,*N*-diphenylaniline (5 g, 15.4 mmol) was dissolved in THF (80 mL) at −78 °C, and *n*-butyl lithium (11.6 mL, 18.5 mmol, 1.6 M in *n*-hexane) was added dropwise using a syringe. After stirring for 1 hour at −78 °C, **1** (2.8 g, 15.4 mmol) in THF (50 mL) was added slowly over a period of 30 min. The resulting mixture was stirred for 2 hours at −78 °C, and the mixture was gradually warmed to room temperature overnight. The reaction was quenched with water, and the product was extracted with EtOAc (3 × 50 mL). Then the organic layer was separated and dried over sodium sulfate (Na_2SO_4). The removal of the solvent under reduced pressure afforded the crude product as a light yellow oil, which was directly used in the next reaction without further purification.

The crude product was dissolved in acetic acid (100 mL) at 110 °C and 10 mL of hydrochloric acid was added dropwise. The mixture was heated to reflux overnight. Then the reaction system was cooled down to room temperature. After the removal of the solvent, the raw product was purified by column chromatography using petroleum ether/EtOAc (3/1, v/v) as an eluent to give **SAIP** as a pale-yellow powder (3.8 g, ∼60%). ^{1}H NMR (600 MHz, chloroform-*d*) δ 8.45 (d, J = 2.6 Hz, 1H), 8.29 (d, J = 2.6 Hz, 1H), 8.19–8.10 (m, 1H), 7.68 (t, J = 7.6 Hz, 2H), 7.60–7.47 (m, 6H), 6.94 (ddd, J = 8.4, 7.1, 1.5 Hz, 2H), 6.57 (t, J = 7.5 Hz, 2H), 6.40 (d, J = 8.4 Hz, 2H), 6.31 (dd, J = 7.9, 1.5 Hz, 2H) ppm. ^{13}C NMR (151 MHz, chloroform-*d*) δ 168.45, 154.67, 152.18, 143.36, 142.76, 141.79, 141.02, 136.86, 131.62, 131.27, 130.94, 128.58, 128.43, 127.83, 127.23, 126.55, 121.77, 121.44, 120.41, 115.17, 55.34 ppm. MALDI-TOF (*m*/*z*), calculated for: 409.492, found: 407.994. Anal. calcd for: $C_{29}H_{19}N_3$ (%): C, 85.06; H, 4.68; N, 10.26; found: C, 85.09; H, 4.72; N, 10.18.

10-Phenyl-10*H*-spiro[acridine-9,11′-indeno[1,2-*b*]quinoxaline] (**SAIQ**) and 10-phenyl-10*H*-spiro[acridine-9,13′-benzo[*g*]indeno-[1,2-*b*]quinoxaline] (**SABIQ**) were prepared by a similar method to that used for **SAIP**.

SAIQ. Bright yellow solid (68%). ^{1}H NMR (600 MHz, chloroform-*d*) δ 8.34–8.29 (m, 1H), 8.14 (d, J = 8.2 Hz, 1H), 7.99 (d, J = 8.3 Hz, 1H), 7.75–7.67 (m, 3H), 7.67–7.55 (m, 7H), 6.95 (t, J = 8.5 Hz, 2H), 6.56 (t, J = 8.1 Hz, 2H), 6.45 (d, J = 8.4 Hz, 2H), 6.37 (d, J = 7.8 Hz, 2H) ppm. ^{13}C NMR (151 MHz, chloroform-*d*) δ 167.72, 154.61, 153.28, 142.62, 142.09, 141.77, 141.12, 136.64, 132.73, 131.31, 130.92, 129.77, 129.43, 128.95, 128.83, 128.63, 128.44, 127.76, 127.42, 126.80, 123.08, 122.06, 120.40, 115.14, 55.16 ppm. MALDI-TOF (*m*/*z*), calculated for: 459.552, found: 458.343. Anal. calcd for: $C_{33}H_{21}N_3$ (%): C, 86.25; H, 4.61; N, 9.14; found: C, 86.30; H, 4.75; N, 9.10.

SABIQ. Orange-yellow solid (62%). ^{1}H NMR (600 MHz, chloroform-*d*) δ 8.69 (s, 1H), 8.53 (s, 1H), 8.39–8.36 (m, 1H), 8.08 (d, J = 8.2 Hz, 1H), 8.00 (d, J = 8.1 Hz, 1H), 7.75 (t, J = 7.7 Hz, 2H), 7.71–7.67 (m, 2H), 7.66–7.57 (m, 4H), 7.55–7.49 (m, 2H), 6.96 (t, J = 8.5 Hz, 2H), 6.58 (t, J = 8.0 Hz, 2H), 6.47 (d, J = 8.5 Hz, 2H), 6.43 (d, J = 7.9 Hz, 2H) ppm. ^{13}C NMR (151 MHz, chloroform-*d*) δ 168.16, 154.57, 154.36, 141.66, 141.12, 139.29, 138.84, 136.62, 133.65, 133.37, 133.16, 131.35, 130.96, 128.99, 128.48, 128.28 (d, J = 6.3 Hz), 127.98, 127.76 (d, J = 13.5 Hz), 127.02 (d, J = 7.0 Hz), 126.51, 126.37, 123.33, 122.27, 120.45, 115.15, 55.06 ppm. MALDI-TOF (*m*/*z*), calculated for: 509.612, found: 509.169. Anal. calcd for: $C_{37}H_{23}N_3$ (%): C, 87.20; H, 4.55; N, 8.25; found: C, 87.34; H, 4.61; N, 8.13.

Results and discussion

Preparation and characterization

The synthesis routes to **SAIP**, **SAIQ**, and **SABIQ** are outlined in Scheme 1. The key precursors **1**,[29] **2**,[36] and **3**[37] were synthesized according to literature methods that provided good yields. Then the ketones underwent nucleophilic addition with 2-lithium-*N*,*N*-diphenylaniline to give the corresponding tertiary alcohols. The subsequent acid catalyzed cyclization produced the target products **SAIP**, **SAIQ**, and **SABIQ** in moderate yields. In addition, ^{1}H and ^{13}C nuclear magnetic resonance (^{1}H/^{13}C NMR), mass spectrometry (MS) and elemental analysis (EA) were utilized to further validate the structures of **SAIP**, **SAIQ**, and **SABIQ**.

Thermal properties

The thermal properties of **SAIP**, **SAIQ**, and **SABIQ** were investigated by differential scanning calorimetry (DSC) and thermogravimetric analysis (TGA) in nitrogen. The experimental results are shown in Fig. 4 and the detailed data are listed in Table 1.

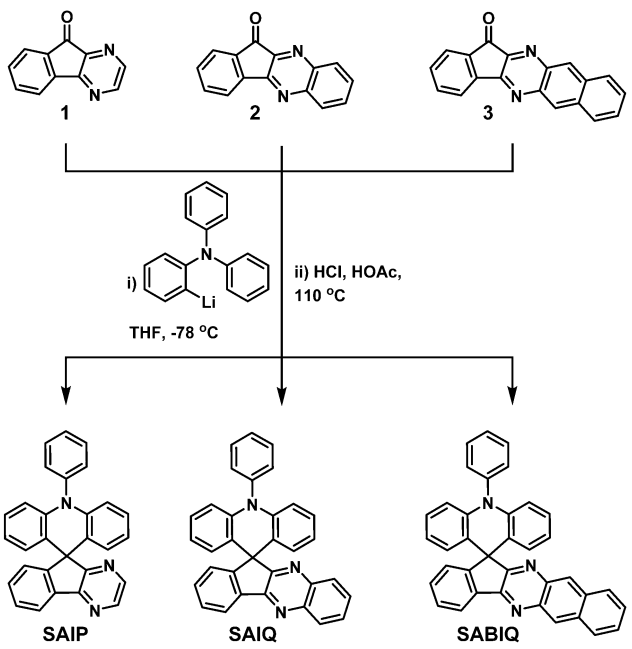

Scheme 1 Synthetic routes to **SAIP**, **SAIQ**, and **SABIQ**.

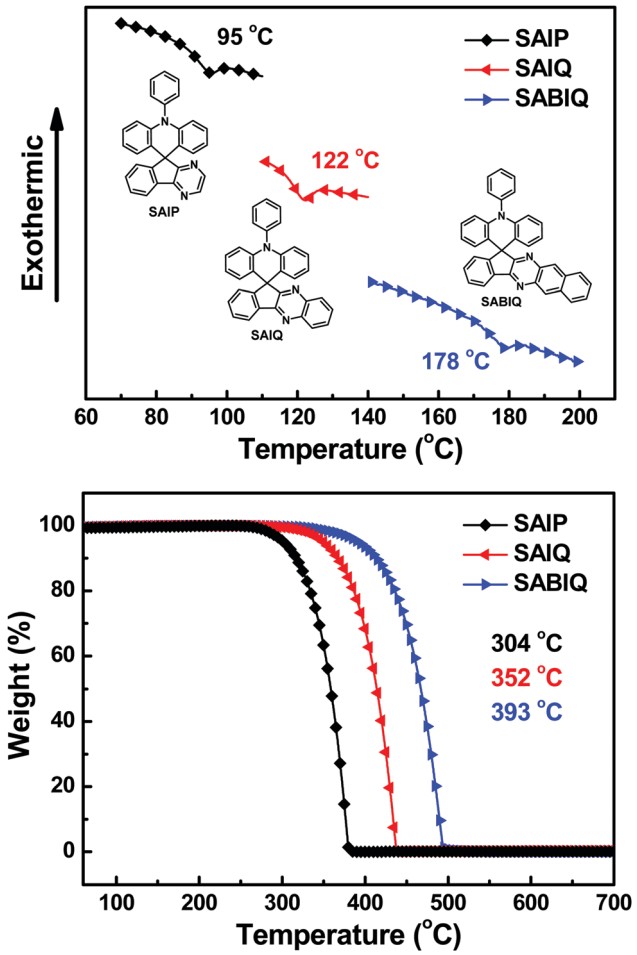

Fig. 4 DSC and TGA curves of **SAIP**, **SAIQ**, and **SABIQ**.

The glass transition temperatures (T_gs) and decomposition temperatures (T_ds, 5 wt% weight loss) were found to be 95, 122 and 178 °C and 304, 352 and 393 °C for **SAIP**, **SAIQ**, and **SABIQ**, respectively. The good thermal properties of these three materials might be due to the rigid and bulky molecular platforms of the spiro-structures. It is worth noting that the nearly 100% weight loss at 381 °C, 439 °C, and 495 °C for **SAIP**, **SAIQ**, and **SABIQ**, respectively, could be due to the sublimation of these compounds.

Photophysical properties

The UV-Vis absorption and photoluminescence (PL) spectra of **SAIP**, **SAIQ**, and **SABIQ** were recorded at room temperature in a dichloromethane (DCM) solution, and phosphorescence (Phos) spectra were recorded at 77 K in a toluene glass matrix (Fig. 5 and Fig. S1, ESI†). Their photophysical results are summarized in Table 1. According to the UV-Vis absorption spectra, the maximum absorption peaks were observed at 321 nm, 348/366 nm, and 374/394 nm for **SAIP**, **SAIQ**, and **SABIQ**, respectively. In addition, the energy gaps (E_gs) are calculated based on the absorption edge, which are 3.58 eV, 3.30 eV, and 2.92 eV for **SAIP**, **SAIQ**, and **SABIQ**, respectively. On the other hand, we can clearly see that the PL spectra of **SAIP**, **SAIQ**, and **SABIQ** are broader and structureless, and their emission peaks were at 478 nm, 539 nm, and 570 nm, respectively. In contrast, the Phos spectra of **SAIP**, **SAIQ**, and **SABIQ** are well-defined (Fig. S1, ESI†), and the corresponding triplet energies (E_Ts) were determined from the first emission peaks in the Phos spectra to be 2.71 eV for **SAIP**, 2.47 eV for **SAIQ**, and 2.38 eV for **SABIQ**. It is noteworthy that from pyrazine to quinoxaline to benzo[*g*]quinoxaline, the π-conjugation systems are extending gradually, which make a direct contribution to the red-shift of their absorption and emission spectra, and the narrowing of their E_gs. In addition, the molecular configuration of **SAIP** resembles that of 10-phenyl-10*H*-spiro[acridine-9,9′-fluorene] (**SAF**),[38] but the triplet energy of **SAIP** is not as high as that of **SAF** (2.87 eV).[38c] The replacement of benzene with pyrazine could be the reason for the reduction in the triplet state energy,[39] but the introduction of the electron-withdrawing group might be beneficial for achieving a more balanced charge transport characteristic, thus resulting in an efficient PHOLED.[35]

In an attempt to understand the electronic structures of the excited states of **SAIP**, **SAIQ**, and **SABIQ**, natural transition orbital (NTO) analysis was used to study the nature of singlet (S_1) and triplet (T_1) excitations of these molecules.[40] As shown in Fig. S2 (ESI†), the holes of the S_1 states of **SAIP**, **SAIQ**, and **SABIQ** were mainly localized at the acridine unit. However, the particles of these three molecules were confined to the electron acceptors, 9*H*-indeno[1,2-*b*]pyrazine, 11*H*-indeno[1,2-*b*]quinoxaline, and 13*H*-benzo[*g*]indeno[1,2-*b*]quinoxaline, which indicate the charge transfer (CT) characteristics of the S_1 states of these compounds. The solvation effect of **SAIP**, **SAIQ**, and **SABIQ** could support their intramolecular charge transfer (ICT) features (Fig. S3, ESI†).[41] Furthermore, for the T_1 state, the holes and particles of **SAIP** and **SAIQ** were similar to those of S_1, but the holes were partially delocalized over pyrazine to a certain extent, which exhibited CT and locally excited (LE) hybrid state characteristics. However, the holes and particles of **SABIQ** were

Table 1 Summary of the physical properties of **SAIP**, **SAIQ**, and **SABIQ**

Molecule	Abs λ_{max}[a] [nm]	PL λ_{max}[a] [nm]	T_g[b]/T_d[c] [°C]	E_g[d] [eV]	E_T[e] [eV]	HOMO[f] [eV]	LUMO[g] [eV]
SAIP	321	478	95/304	3.58	2.71	−5.33	−1.75
SAIQ	348, 366	539	122/352	3.30	2.47	−5.33	−2.03
SABIQ	374, 394	570	178/393	2.92	2.38	−5.34	−2.42

[a] Measured in dichloromethane solution at room temperature. [b] T_g: glass transition temperature. [c] T_d: decomposition temperature. [d] E_g: optical band gap energies were calculated from the corresponding absorption onset in dichloromethane solution. [e] E_T: measured in a toluene glass matrix at 77 K. [f] HOMO levels were calculated from CV data. [g] LUMO levels were calculated from the HOMOs and E_gs.

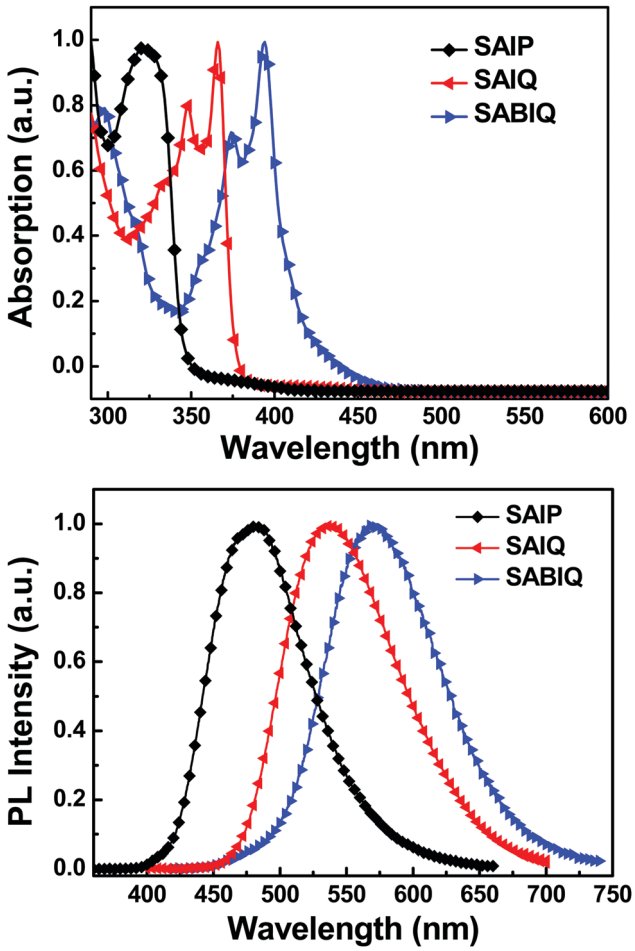

Fig. 5 UV-Vis absorption and PL spectra of **SAIP**, **SAIQ**, and **SABIQ**.

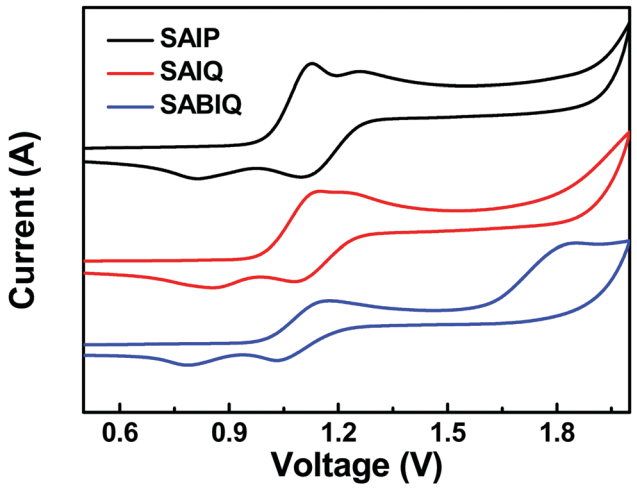

Fig. 6 Cyclic voltammograms of **SAIP**, **SAIQ**, and **SABIQ**.

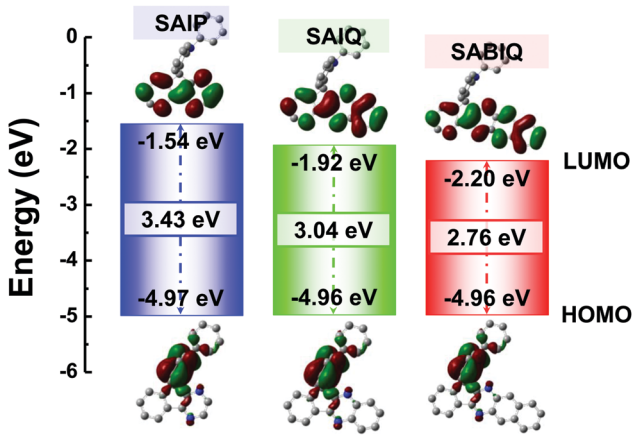

Fig. 7 Frontier molecular orbital distributions and energy levels of **SAIP**, **SAIQ**, and **SABIQ**.

mainly localized at the benzo[*g*]quinoxaline motif, which demonstrated an LE state characteristic.

Electrochemical properties and theoretical calculations

The HOMO and LUMO energy levels of a host play an important role in device fabrication and optimization. Therefore, we investigated the electrochemical behaviors of **SAIP**, **SAIQ**, and **SABIQ** by cyclic voltammetry (CV). The HOMO energy levels can be estimated from the onset of oxidation waves. As shown in Fig. 6, the electrochemical behaviors of **SAIP**, **SAIQ**, and **SABIQ** were alike at the onset of the oxidation waves around 1.0 V. Therefore, **SAIP**, **SAIQ**, and **SABIQ** exhibited very similar HOMO energy levels. On the other hand, the LUMO energy levels of **SAIP** (−1.75 eV), **SAIQ** (−2.03 eV), and **SABIQ** (−2.42 eV) can be calculated by subtracting the optical energy gaps (E_gs) from the corresponding HOMO energy levels. Furthermore, we also studied the frontier molecular orbital (FMO) electronic distributions and the energy levels of **SAIP**, **SAIQ**, and **SABIQ** using density function theory (DFT) calculations at the B3LYP/6-31G(d) level. As illustrated in Fig. 7, the HOMOs were mainly distributed on the electron rich acridine motifs, which led to **SAIP**, **SAIQ**, and **SABIQ** having almost the same HOMO energy level. The LUMOs reside over the diaza-containing motifs in these compounds. From **SAIP** to **SAIQ** and to **SABIQ**, the E_gs decrease gradually with the extension of molecular π-conjugation, and the LUMO energy levels decrease as well.

Electroluminescence properties

In order to investigate the electroluminescence (EL) properties of these novel spirocycles, blue, green and red PHOLEDs were fabricated with the following device configurations: ITO/HAT-CN (10 nm)/TAPC (55 nm)/TCTA (10 nm)/**SAIP:** 10 wt% FIrpic (20 nm)/B4PyMPM (45 nm)/Liq (2 nm)/Al (120 nm) (blue device, denoted as B1), ITO/HAT-CN (10 nm)/TAPC (55 nm)/**SAIP** or **SAIQ:** 10 wt% $Ir(ppy)_2(acac)$ (20 nm)/B4PyMPM (40 nm)/Liq (2 nm)/Al (120 nm) (green device, denoted as G1 or G2), and ITO/HAT-CN (10 nm)/TAPC (45 nm)/TCTA (10 nm)/**SAIP** or **SAIQ:** 6 wt% $Ir(MDQ)_2(acac)$ (20 nm)/TmPyPB (45 nm)/Liq (2 nm)/Al (120 nm) (red device, denoted as R1 or R2). Fig. 8, 9 and Fig. S5 (ESI†) show the current density–voltage–luminance (*J*–*V*–*L*) characteristics, current efficiency (CE)/power efficiency (PE)/external quantum efficiency (EQE)–*L* curves, and EL spectra of the corresponding PHOLEDs. These device parameters are listed in Table 2.

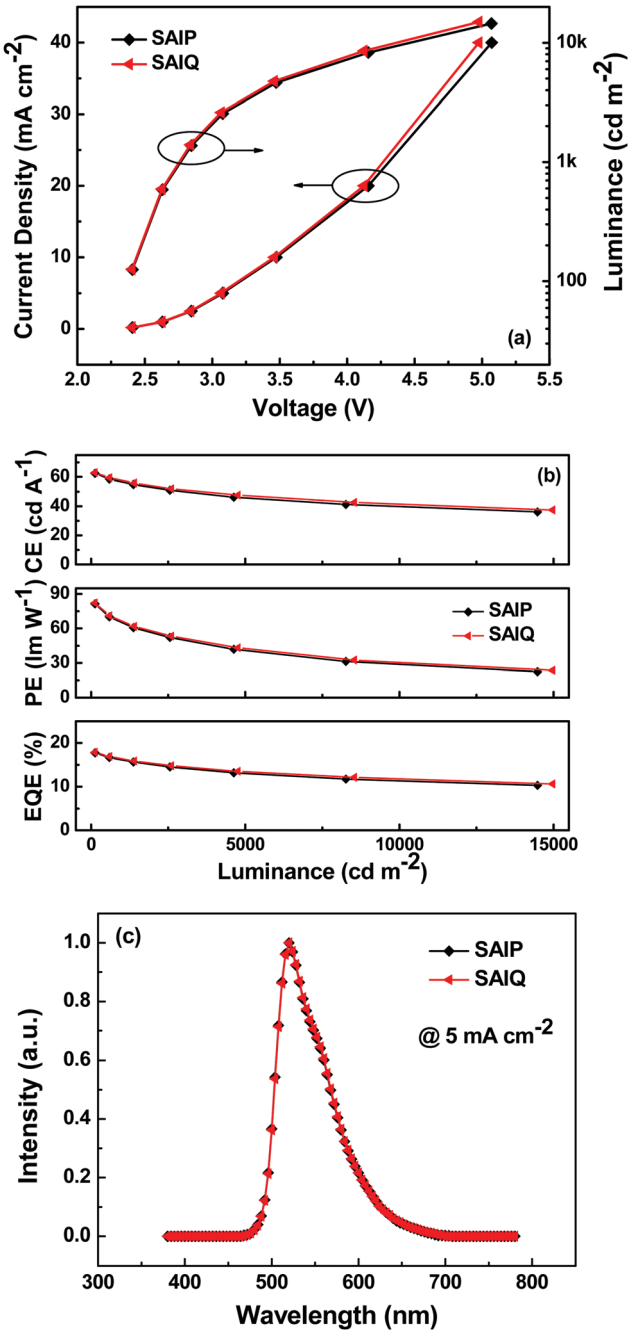

Fig. 8 (a) *J*–*V*–*L* characteristics, (b) CE–, PE–, and EQE–*L* curves, and (c) EL spectra of the green devices.

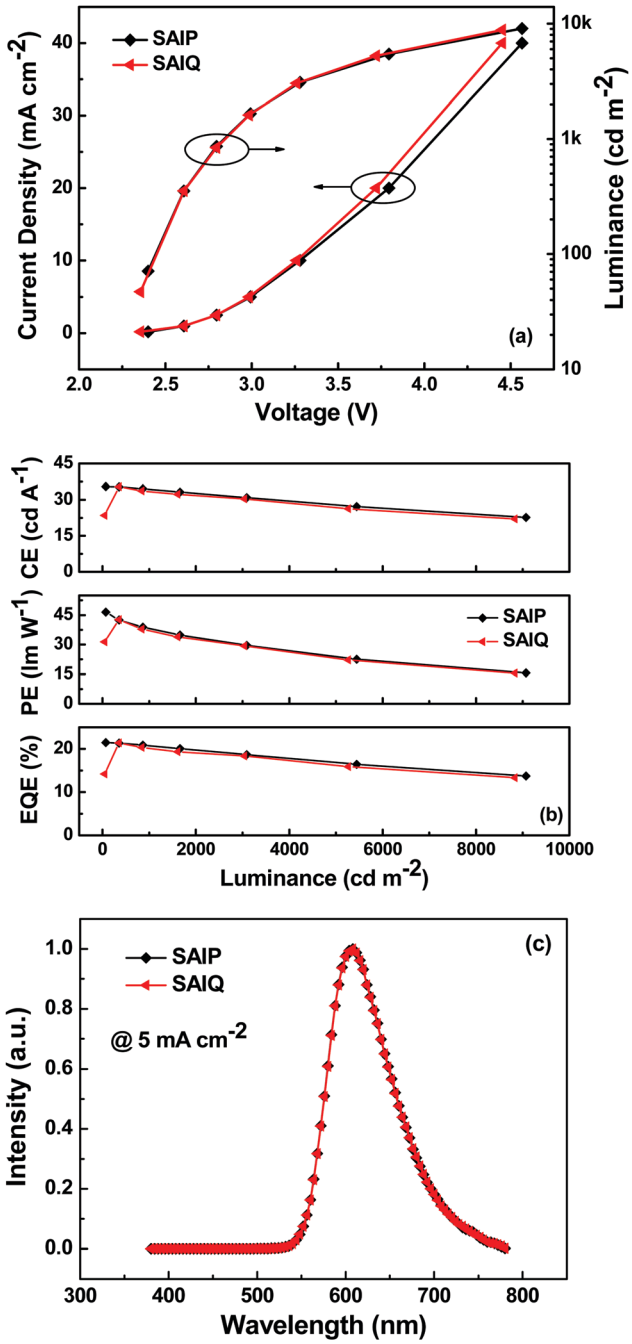

Fig. 9 (a) *J*–*V*–*L* characteristics, (b) CE–, PE–, and EQE–*L* curves, and (c) EL spectra of the red devices.

The green and red devices based on **SAIP** and **SAIQ** exhibited very similar device performances. More specifically, the **SAIP** and **SAIQ** based green and red devices showed relatively low driving voltages (2.5 V) at a brightness of 200 cd m^{-2}. Furthermore, the green and red devices also demonstrated relatively high device efficiencies. The maximum CE/PE/EQE achieved were 62.5 cd A^{-1}/81.5 lm W^{-1}/17.8% and 63.0 cd A^{-1}/82.3 lm W^{-1}/17.9% for the **SAIP** and **SAIQ** hosted green devices, respectively. The maximum CE, PE, and EQE could reach 35.5/35.4 cd A^{-1}, 46.5/42.6 lm W^{-1}, and 21.5%/21.4% for the **SAIP**/**SAIQ** based red devices, respectively. The Commission Internationale de l'Eclairage (CIE) coordinates of the **SAIP** and **SAIQ** based green and red devices are (0.32, 0.63) and (0.61, 0.39), respectively, which are consistent with those of the reported $Ir(ppy)_2(acac)$[42] and $Ir(MDQ)_2(acac)$[43] doped devices. For the **SAIP** and **SAIQ** hosted devices, there are some factors that can account for their similar device performance. The high E_Ts of **SAIP** and **SAIQ** would result in an efficient energy transfer process from the host to the dopant, and prevent reverse energy transfer from the dopant to the host.[44] Moreover, suitable HOMO/LUMO energy

Table 2 Electroluminescence characteristics of the blue, green, and red devices

Device[a]	Host	V^b [V]	$\eta_{CE}{}^c$ [cd A^{-1}]	$\eta_{PE}{}^c$ [lm W^{-1}]	EQE[c] [%]	CIE[d] [x, y]
B1	**SAIP**	2.6	22.0, 18.7	28.0, 20.9	11.0, 9.4	0.16, 0.33
G1	**SAIP**	2.5	62.5, 59.7	81.5, 71.8	17.8, 16.7	0.32, 0.63
G2	**SAIQ**	2.5	63.0, 60.6	82.3, 73.6	17.9, 17.4	0.32, 0.63
R1	**SAIP**	2.5	35.5, 35.1	46.5, 41.7	21.5, 21.2	0.61, 0.39
R2	**SAIQ**	2.5	35.4, 35.0	42.6, 41.2	21.4, 21.0	0.61, 0.39

[a] Device configuration: B1: ITO/HAT-CN (10 nm)/TAPC (55 nm)/TCTA (10 nm)/**SAIP**: 10 wt% FIrpic (20 nm)/B4PyMPM (45 nm)/Liq (2 nm)/Al (120 nm); G1/G2: ITO/HAT-CN (10 nm)/TAPC (55 nm)/**SAIP** or **SAIQ**: 10 wt% $Ir(ppy)_2(acac)$ (20 nm)/B4PyMPM (40 nm)/Liq (2 nm)/Al (120 nm); and R1/R2: ITO/HAT-CN (10 nm)/TAPC (45 nm)/TCTA (10 nm)/**SAIP** or **SAIQ**: 6 wt% $Ir(MDQ)_2(acac)$ (20 nm)/TmPyPB (45 nm)/Liq (2 nm)/Al (120 nm). [b] Voltages at 200 cd m^{-2}. [c] Efficiencies in the order of the maxima and at 500 cd m^{-2}. [d] Commission Internationale de l'Eclairage coordinates measured at 5 mA cm^{-2}.

levels of **SAIP** and **SAIQ** would reduce the hole and electron injection barrier, thus lowering the device driving voltages and achieving a high PE. In addition, the good thermal stabilities of **SAIP** and **SAIQ** will be favorable for the device operation stability. In addition, the PLQYs of $Ir(PPy)_2(acac)$ (10 wt%) and $Ir(MDQ)_2(acac)$ (6 wt%) in **SAIP**/**SAIQ** were measured to be 66%/69% and 75%/74%, respectively, which were consistent with the observed EQEs for the **SAIP** (green, 17.8%; red, 21.5%) and **SAIQ** (green, 17.9%; red, 21.4%) hosted devices. These results further suggest that **SAIP** and **SAIQ** could effectively confine the triplet energies of green and red dopants within devices. On the other hand, hole-only and electron-only devices were fabricated to study the charge transport properties of **SAIP** and **SAIQ** with the following device structures: hole-only devices, ITO/MoO_3 (10 nm)/**SAIP** or **SAIQ** (100 nm)/MoO_3 (10 nm)/Al (100 nm); electron-only: ITO/TmPyPB (20 nm)/**SAIP** or **SAIQ** (100 nm)/TmPyPB (20 nm)/Liq (2 nm)/Al (100 nm) (Fig. 10). Both **SAIP** and **SAIQ** demonstrated the bipolar transport character with similar hole and electron mobilities, which could account in part for their similar device performance. In addition, the hole- and electron-mobility of **SAIP** and **SAIQ** were estimated according to the literature method[45] to be $\mu_{SAIP,h} = 6.2 \times 10^{-5}$ cm V^{-1} s^{-1}, $\mu_{SAIP,e} = 1.3 \times 10^{-7}$ cm V^{-1} s^{-1}; $\mu_{SAIQ,h} = 5.7 \times 10^{-5}$ cm V^{-1} s^{-1}, and $\mu_{SAIQ,e} = 3.2 \times 10^{-7}$ cm V^{-1} s^{-1}. Thus, detailed studies of the relationships between molecular structures, physical/chemical properties, and device performance are important. As shown in Fig. S5 (ESI†), the performance of the **SAIP** hosted blue device was relatively low compared with those of the corresponding green and red devices. The maximum CE, PE, and EQE were 22.0 cd A^{-1}, 28.0 lm W^{-1}, and 11.0%, respectively. This result is not satisfactory, probably due to the small E_T difference between **SAIP** (2.71 eV) and the blue dopant FIrpic (2.62 eV),[31b] which could favor the reverse energy transfer from the dopant to the host, although the emission from the host was not observed in the EL spectrum.

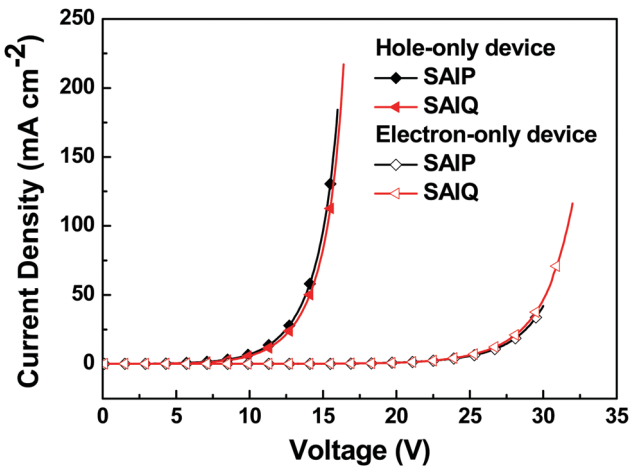

Fig. 10 Hole- and electron-only devices based on **SAIP** and **SAIQ**.

Conclusions

In conclusion, three novel spirocycle compounds (**SAIP**, **SAIQ**, and **SABIQ**) containing an electron donating acridine unit and an electron withdrawing pyrazine segment were designed and synthesized. The different π-conjugation lengths of the acceptor units led to the different photophysical properties of **SAIP**, **SAIQ**, and **SABIQ**. Our results show that the green and red PHOLEDs exhibit a similar and relatively high device performance with those of **SAIP** and **SAIQ** as host materials. The maximum EQE of the green and red devices could exceed 17% and 21%, respectively. Correspondingly, we hope our study will expand the application of 1,4-diazafluorenone and its analogues in the field of OLED materials and shed new light on the development of efficient host materials.

Conflicts of interest

There are no conflicts to declare.

Acknowledgements

We acknowledge financial support from the National Key R&D Program of China (2016YFB0400703), the National Natural Science Foundation of China (21472135, 61307036), the Natural Science Foundation of Jiangsu Province of China (BK20151216), and the 111 Project. This project is also funded by the Collaborative Innovation Center of Suzhou Nano Science and Technology (CIC-Nano), Soochow University and by the Priority Academic Program Development of Jiangsu Higher Education Institutions (PAPD).

References

1 (*a*) N. S. Prostakov, *Usp. Khim.*, 1969, **38**, 1710 (*Russ. Chem. Rev.*, 1969, **38**, 774); (*b*) C. Mayor and C. Wentrup, *J. Am. Chem. Soc.*, 1975, **97**, 7464; (*c*) N. S. Prostakov, A. T. Soldatenkov, N. M. Kolyadina and A. A. Obynochnyi, *Russ. Chem. Rev.*, 1997, **66**, 121.

2 (*a*) O. Doebner and P. Kuntze, *Ann. Chem.*, 1988, **249**, 109; (*b*) O. Doebner and J. Peters, *Ber. Dtsch. Chem. Ges.*, 1890,

23, 1228; (*c*) R. Oberkobusch, *Ber.*, 1953, **86**, 975; (*d*) K. Kloc, J. Mlochowski and Z. Szulc, *J. Prakt. Chem.*, 1977, **319**, 959.

3 (*a*) V. Petrov, J. Saper and B. Sturgeon, *J. Chem. Soc.*, 1949, 2134; (*b*) J. N. Chatterjea, S. C. Shaw and S. N. Singh, *Indian J. Chem.*, 1978, **55**, 149; (*c*) E. Y. Ozola and G. Y. Vanag, *Khim. Geterotsikl. Soedin.*, 1969, **5**, 103 (*Chem. Heterocycl. Compd.*, 1969, **5**, 82); (*d*) Y. E. Pelcher, A. K. Aren, Z. A. Bomika and G. Y. Vanag, *Khim. Geterotsikl. Soedin.*, 1969, **5**, 305 (*Chem. Heterocycl. Compd.*, 1969, **5**, 232).

4 (*a*) B. A. Vigante, Y. Ozols, E. M. Belash and Y. I. Beilis, *Khim. Geterotsikl. Soedin.*, 1984, **2**, 210 (*Chem. Heterocycl. Compd.*, 1984, **20**, 170); (*b*) Y. Ozols, B. A. Vigante and G. Y. Dubur, *Geterotsikl. Soedin.*, 1994, 1603 (*Chem. Heterocycl. Compd.*, 1994, **20**, 1386); (*c*) R. Ulrich, *J. Heterocycl. Chem.*, 1990, **27**, 237.

5 (*a*) J. Beger and W. Triebs, *Ann. Chem.*, 1962, **652**, 204; (*b*) N. S. Prostakov, L. M. Kirillova, D. Pkhal'gumani, L. A. Shakhparonova and V. P. Zvolinskii, *Khim. Geterotsikl. Soedin.*, 1967, **3**, 1068 (*Chem. Heterocycl. Compd.*, 1967, **3**, 832); (*c*) N. S. Prostakov, O. I. Sorokin and A. Y. Ismailov, *Khim. Geterotsikl. Soedin.*, 1967, **3**, 674 (*Chem. Heterocycl. Compd.*, 1967, **3**, 541); (*d*) M.-J. Shiao, C.-J. Peng, J.-S. Wang and Y.-T. Ma, *J. Chin. Chem. Soc.*, 1992, **39**, 173; (*e*) A.-S. Rebstock, F. Mongin, F. Trécourt and G. Quéguiner, *Tetrahedron*, 2003, **59**, 4973; (*f*) D. Tilly, A.-S. Castanet and J. Mortier, *Tetrahedron Lett.*, 2006, **47**, 1121.

6 J. T. Plati, A. K. Ingberman and W. Wenner, *J. Org. Chem.*, 1957, **22**, 2615.

7 (*a*) B. F. Bowden, K. Picker, R. Ritchie and W. C. Taylor, *Aust. J. Chem.*, 1975, **28**, 2681; (*b*) J. C. Powers and I. Ponticello, *J. Am. Chem. Soc.*, 1968, **90**, 7102; (*c*) M. J. Shiao, K. H. Liu and P. Y. Lin, *Heterocycles*, 1993, **36**, 507; (*d*) M. T. Du Priest, C. L. Schmidt, D. Kuzmich and S. B. Willams, *J. Org. Chem.*, 1986, **51**, 2021.

8 M. Alessi, A. L. Larkin, K. A. Ogilvie, L. A. Green, S. Lai, S. Lopez and V. Snieckus, *J. Org. Chem.*, 2007, **72**, 1588.

9 W. H. Mills, W. H. Palmer and M. G. Tomkinson, *J. Chem. Soc.*, 1924, 2364.

10 R. H. Prager, C. Tsopelas and T. Heisler, *Aust. J. Chem.*, 1991, **44**, 227.

11 L. M. Yagupolskii, K. I. Petko, A. N. Retchitsky and I. I. Maletina, *J. Fluorine Chem.*, 1994, **67**, 5.

12 R. C. Fuson and J. J. Miller, *J. Am. Chem. Soc.*, 1957, **79**, 3477.

13 E. P. Kyba, S.-T. Liu, K. Chockalingam and B. R. Reddy, *J. Org. Chem.*, 1988, **53**, 3513.

14 J. W. Lockner, D. D. Dixon, R. Risgaard and P. S. Baran, *Org. Lett.*, 2011, **13**, 5628.

15 (*a*) D. Mueller, R. A. Davis, S. Duffy, V. M. Avery, D. Camp and R. J. Quinn, *J. Nat. Prod.*, 2009, **72**, 1538; (*b*) S. Dhara, A. Ahmed, S. Nandi, S. Baitalik and J. K. Ray, *Tetrahedron Lett.*, 2013, **54**, 63; (*c*) N. Marquise, V. Dorcet, F. Chevallier and F. Mongin, *Org. Biomol. Chem.*, 2014, **12**, 8138; (*d*) N. Marquise, P. J. Harford, F. Chevallier, T. Roisnel, A. E. H. Wheatley, P. C. Gros and F. Mongin, *Tetrahedron Lett.*, 2013, **54**, 3154; (*e*) N. Marquise, P. J. Harford, F. Chevallier, T. Roisnel, V. Dorcet, A.-L. Gagez, S. Sable, L. Picot, V. Thiery, A. E. H. Wheatley, P. C. Gros and F. Mongin, *Tetrahedron*, 2013, **69**, 10123.

16 J. K. Laha, K. P. Jethava and S. Patel, *Org. Lett.*, 2015, **17**, 5890.

17 J. K. Laha, K. P. Jethava, S. Patel and K. V. Patel, *J. Org. Chem.*, 2017, **82**, 76.

18 (*a*) S.-J. Su, C. Cai and J. Kido, *Chem. Mater.*, 2011, **23**, 274; (*b*) S.-J. Su, C. Cai and J. Kido, *J. Mater. Chem.*, 2012, **22**, 3447; (*c*) D. Chen, S.-J. Su and Y. Cao, *J. Mater. Chem. C*, 2014, **2**, 9565.

19 (*a*) Q. Yan, E. Gin, M. G. Banwell, A. C. Willis and P. D. Carr, *J. Org. Chem.*, 2017, **82**, 4328; (*b*) Y. Im and J. Y. Lee, *Chem. Commun.*, 2013, **49**, 5948; (*c*) T. Motoyama, H. Sasabe, Y. Seino, J. Takamatsu and J. Kido, *Chem. Lett.*, 2011, **40**, 306; (*d*) S. J. Kim, Y. J. Kim, Y. H. Son, J. A. Hur, H. A. Um, J. Shin, T. W. Lee, M. J. Cho, J. K. Kim, S. Joo, J. H. Yang, G. S. Chae, K. Choi, J. H. Kwon and D. H. Choi, *Chem. Commun.*, 2013, **49**, 6788; (*e*) E. Varathan, D. Vijay and V. Subramanian, *J. Phys. Chem. C*, 2014, **118**, 21741; (*f*) Z. Zhang, J. Xie, Z. Wang, B. Shen, H. Wang, M. Li, J. Zhang and J. Cao, *J. Mater. Chem. C*, 2016, **4**, 4226; (*g*) J. S. Moon, D. H. Ahn, S. W. Kim, S. Y. Lee, J. Y. Lee and J. H. Kwon, *RSC Adv.*, 2018, **8**, 17025.

20 (*a*) C. W. Lee, J.-K. Kim, S. H. Joo and J. Y. Lee, *ACS Appl. Mater. Interfaces*, 2013, **5**, 2169; (*b*) C. W. Lee and J. Y. Lee, *Adv. Mater.*, 2013, **25**, 596; (*c*) M.-M. Xue, C.-C. Huang, Y. Yuan, Y.-X. Zhang, M.-K. Fung and L.-S. Liao, *Chem. Commun.*, 2017, **53**, 263; (*d*) J. H. Kim, D. R. Lee, S. H. Han and J. Y. Lee, *J. Mater. Chem. C*, 2018, **6**, 5363.

21 C. W. Lee and J. Y. Lee, *Chem. Commun.*, 2013, **49**, 1446.

22 (*a*) P. Wu, J. Zhu, Z. Zhang, D. Dou, H. Wang, B. Wei and Z. Wang, *Dyes Pigm.*, 2018, **156**, 185; (*b*) S. Jeong, C. Kim, S. H. Kim, D. Y. Kim, S. E. Lee, Y. K. Kim and S. S. Yoon, *Mol. Cryst. Liq. Cryst.*, 2018, **660**, 24; (*c*) H.-F. Chen, W.-Y. Hung, S.-W. Chen, T.-C. Wang, S.-W. Lin, S.-H. Chou, C.-T. Liao, H.-C. Su, H.-A. Pan, P.-T. Chou, Y.-H. Liu and K.-T. Wong, *Inorg. Chem.*, 2012, **51**, 12114; (*d*) K.-T. Wong, T.-Y. Hwu, A. Balaiah, T.-C. Chao, F.-C. Fang, C.-T. Lee and Y.-C. Peng, *Org. Lett.*, 2006, **8**, 1415; (*e*) M. L. Keshtova, S. I. Pozinb, D. V. Marochkinc, V. P. Perevalovc, P. V. Petrovskiia, I. V. Blagodatskikha and A. A. R. Khokhlova, *Dokl. Chem.*, 2012, **442**, 50; (*f*) K.-T. Wong, R.-T. Chen, F.-C. Fang, C.-c. Wu and Y.-T. Lin, *Org. Lett.*, 2005, **7**, 1979; (*g*) H.-C. Liao, C.-H. Lee, Y.-C. Ho, M.-H. Jao, C.-M. Tsai, C.-M. Chuang, J.-J. Shyue, Y.-F. Chen and W.-F. Su, *J. Mater. Chem.*, 2012, **22**, 10589; (*h*) K.-T. Wong, H.-F. Chen and F.-C. Fang, *Org. Lett.*, 2006, **8**, 3501; (*i*) Z. Jiang, H. Yao, Z. Zhang, C. Yang, Z. Liu, Y. Tao, J. Qin and D. Ma, *Org. Lett.*, 2009, **11**, 2607; (*j*) C. Fan, Y. Chen, P. Gan, C. Yang, C. Zhong, J. Qin and D. Ma, *Org. Lett.*, 2010, **12**, 5648.

23 H.-C. Su, F.-C. Fang, T.-Y. Hwu, H.-H. Hsieh, H.-F. Chen, G.-H. Lee, S.-M. Peng, K.-T. Wong and C.-C. Wu, *Adv. Funct. Mater.*, 2007, **17**, 1019.

24 L.-L. Yang and Q.-C. Liu, *Chin. J. Synth. Chem.*, 2011, **19**, 73.

25 A. Mustafa, N. M. Mikhailova, N. I. Golovtsov and N. S. Prostakov, *Chem. Heterocycl. Compd.*, 1992, **28**, 1155.

26 (*a*) J. Druey and P. Schmidt, *Helv. Chim. Acta*, 1950, **33**, 1080; (*b*) Y.-Z. Li and G. B. Schuster, *J. Org. Chem.*, 1987, **52**, 3975.
27 (*a*) R. Frédérick, W. Dumont, F. Ooms, L. Aschenbach, C. J. Van der Schyf, N. Castagnoli, J. Wouters and A. Krief, *J. Med. Chem.*, 2006, **49**, 3743; (*b*) S. Kneubühler, U. Thull, C. Altomare, V. Carta, P. Gaillard, P.-A. Carrupt, A. Carotti and B. Testa, *J. Med. Chem.*, 1995, **38**, 3874; (*c*) S. Kneubühler, V. Carta, C. Altomare, A. Carotti and B. Testa, *Helv. Chim. Acta*, 1993, **76**, 1956.
28 C. Altomare, S. Cellamare, L. Summo, M. Catto and A. Carotti, *J. Med. Chem.*, 1998, **41**, 3812.
29 A. A. C. Takaizumi, F. R. dos Santos, M. T. Silva and J. C. Netto-Ferreira, *Quim. Nova*, 2009, **32**, 1799.
30 (*a*) Y. Tao, C. Yang and J. Qin, *Chem. Soc. Rev.*, 2011, **40**, 2943; (*b*) R. C. Kwong, S. Sibley, T. Dubovoy, M. Baldo, S. R. Forrest and M. E. Thompson, *Chem. Mater.*, 1999, **11**, 3709; (*c*) C. Adachi, M. A. Baldo, S. R. Forrest, S. Lamansky, M. E. Thompson and R. C. Kwong, *Appl. Phys. Lett.*, 2001, **78**, 1622; (*d*) C. Adachi, M. A. Baldo, M. E. Thompson and S. R. Forrest, *J. Appl. Phys.*, 2001, **90**, 5048; (*e*) M. A. Baldo, S. Lamansky, P. E. Burrows, M. E. Thompson and S. R. Forrest, *Appl. Phys. Lett.*, 1999, **75**, 4; (*f*) S.-J. Su, H. Sasabe, T. I. Takeda and J. Kido, *Chem. Mater.*, 2008, **20**, 1691.
31 (*a*) L.-X. Xiao, Z.-J. Chen, B. Qu, J.-X. Luo, S. Kong, Q.-H. Gong and J. Kido, *Adv. Mater.*, 2011, **23**, 926; (*b*) C. Adachi, R. C. Kwong, P. Djurovich, V. Adamovich, M. A. Baldo, M. E. Thompson and S. R. Forrest, *Appl. Phys. Lett.*, 2001, **79**, 2082; (*c*) R. J. Holmes, S. R. Forrest, Y. J. Tung, R. C. Kwong, J. J. Brown, S. Garon and M. E. Thompson, *Appl. Phys. Lett.*, 2003, **82**, 2422.
32 (*a*) X.-Y. Liu, X. Tang, Y. Zhao, D. Zhao, J. Fan and L.-S. Liao, *ACS Appl. Mater. Interfaces*, 2018, **10**, 1925; (*b*) X.-Y. Liu, X. Tang, Y. Zhao, D. Zhao, J. Fan and L.-S. Liao, *J. Mater. Chem. C*, 2018, **6**, 1023; (*c*) W.-C. Chen, Y. Yuan, Z.-L. Zhu, Z.-Q. Jiang, S.-J. Su, L.-S. Liao and C.-S. Lee, *Chem. Sci.*, 2018, **9**, 4062; (*d*) Y.-K. Wang, S.-H. Li, S.-F. Wu, C.-C. Huang, S. Kumar, Z.-Q. Jiang, M.-K. Fung and L.-S. Liao, *Adv. Funct. Mater.*, 2018, **28**, 1706228; (*e*) D. Liu, F. Wang and R. Yao, *J. Mater. Chem. C*, 2018, **6**, 7839.
33 (*a*) K.-H. Kim, S. Lee, C.-K. Moon, S.-Y. Kim, Y.-S. Park, J.-H. Lee, J. W. Lee, J. Huh, Y. You and J.-J. Kim, *Nat. Commun.*, 2014, **5**, 4769; (*b*) C.-J. Shih, C.-C. Lee, T.-H. Yeh, S. Biring, K. K. Kesavan, N. R. Al Amin, M.-H. Chen, W.-C. Tang, S.-W. Liu and K.-T. Wong, *ACS Appl. Mater. Interfaces*, 2018, **10**, 24090; (*c*) Y. Wang, W. Wang, Z. Huang, H. Wang, J. Zhao, J. Yu and D. Ma, *J. Mater. Chem. C*, 2018, **6**, 7042; (*d*) D. Zhang, J. Qiao, D. Zhang and L. Duan, *Adv. Mater.*, 2017, 1702847; (*e*) M. Bian, D. Zhang, Y. Wang, Y.-H. Chung, Y. Liu, H. Ting, L. Duan, Z. Chen, Z. Bian, Z. Liu and L. Xiao, *Adv. Funct. Mater.*, 2018, 1800429.
34 (*a*) W.-Y. Hung, T.-C. Wang, H.-C. Chiu, H.-F. Chen and K.-T. Wong, *Phys. Chem. Chem. Phys.*, 2010, **12**, 10685; (*b*) H.-F. Chen, T.-C. Wang, W.-Y. Hung, H.-C. Chiu, C. Yun and K.-T. Wong, *J. Mater. Chem.*, 2012, **22**, 9658.
35 (*a*) M. Romain, D. Tondelier, O. Jeannin, B. Geffroy, J. Rault-Berthelot and C. Poriel, *J. Mater. Chem. C*, 2015, **3**, 9701; (*b*) S. Thiery, D. Tondelier, B. Geffroy, O. Jeannin, J. Rault-Berthelot and C. Poriel, *Chem. – Eur. J.*, 2016, **22**, 10136.
36 (*a*) S. Ruhemann, *J. Chem. Soc.*, 1910, **97**, 1438; (*b*) B. D. Pearson, R. A. Mitsch and N. H. Cromwell, *J. Org. Chem.*, 1962, **27**, 1674; (*c*) F. D. Popp, *J. Heterocycl. Chem.*, 1972, **9**, 1399; (*d*) L. W. Deady, J. Desneves and A. C. Ross, *Tetrahedron*, 1993, **49**, 9823.
37 C. Zhang, S. Li, L. Ji, S. Liu, Z. Li, S. Li and X. Meng, *Bioorg. Med. Chem. Lett.*, 2015, **25**, 4693.
38 (*a*) C.-J. Lin, H.-L. Huang, M.-R. Tseng and C.-H. Cheng, *J. Disp. Technol.*, 2009, **5**, 236; (*b*) C.-Y. Chan, Y.-C. Wong, M.-Y. Chan, S.-H. Cheung, S.-K. So and V. W.-W. Yam, *ACS Appl. Mater. Interfaces*, 2016, **8**, 24782; (*c*) W.-C. Chen, Y. Yuan, Z.-L. Zhu, S.-F. Ni, Z.-Q. Jiang, L.-S. Liao, F.-L. Wong and C.-S. Lee, *Chem. Commun.*, 2018, **54**, 4541; (*d*) W. Sun, N. Zhou, Y. Xiao, S. Wang and X. Li, *Chem. – Asian J.*, 2017, **12**, 3069.
39 (*a*) X.-Y. Liu, F. Liang, Y. Yuan, Z.-Q. Jiang and L.-S. Liao, *J. Mater. Chem. C*, 2016, **4**, 7869; (*b*) X.-Y. Liu, F. Liang, L.-S. Cui, X.-D. Yuan, Z.-Q. Jiang and L.-S. Liao, *Chem. – Asian J.*, 2015, **10**, 1402.
40 (*a*) Z. Chen, Z. Wu, F. Ni, C. Zhong, W. Zeng, D. Wei, K. An, D. Ma and C. Yang, *J. Mater. Chem. C*, 2018, **6**, 6543; (*b*) C. Li, X. Fan, C. Han and H. Xu, *J. Mater. Chem. C*, 2018, **6**, 6747.
41 (*a*) N. Mataga, Y. Kaifu and M. Kaizumi, *Bull. Chem. Soc. Jpn.*, 1956, **29**, 465; (*b*) N. G. Bakhshiev, M. I. Knyazhanskii, V. I. Minkin, O. A. Osipov and G. V. Saidov, *Russ. Chem. Rev.*, 1969, **38**, 740; (*c*) Y. Zhang, K. Wang, G. Zhuang, Z. Xie, C. Zhang, F. Cao, G. Pan, H. Chen, B. Zou and Y. Ma, *Chem. – Eur. J.*, 2015, **21**, 2474.
42 S. Lamansky, P. Djurovich, D. Murphy, F. Abdel-Razzaq, H. E. Lee, C. Adachi, E. Paul, P. E. Burrows, S. R. Forrest and M. E. Thompson, *J. Am. Chem. Soc.*, 2001, **123**, 4304.
43 J. P. Duan, P. P. Sun and C. H. Cheng, *Adv. Mater.*, 2003, **15**, 224.
44 J. Zhao, G.-H. Xie, C.-R. Yin, L.-H. Xie, C.-M. Han, R.-F. Chen, H. Xu, M.-D. Yi, Z.-P. Deng, S.-F. Chen, Y. Zhao, S.-Y. Liu and W. Huang, *Chem. Mater.*, 2011, **23**, 5331.
45 (*a*) B. Wang, X. Lv, J. Tan, Q. Zhang, Z. Huang, W. Yi and L. Wang, *J. Mater. Chem. C*, 2016, **4**, 8473; (*b*) J. Tan, B. Wang, Z. Huang, X. Lv, W. Yi, S. Zhuang and L. Wang, *J. Mater. Chem. C*, 2016, **4**, 5222.

